

2D-ELDOR using full S_{c-} fitting and absorption lineshapes

Yun-Wei Chiang¹, Antonio Costa-Filho², Jack H. Freed^{*}

Baker Laboratory of Chemistry and Chemical Biology, National Biomedical ACERT Center for Advanced ESR Technology, Cornell University, Ithaca, NY 14853-1301, USA

Received 7 March 2007; revised 30 May 2007

Available online 13 July 2007

Abstract

Recent progress in developing 2D-ELDOR (2D electron–electron double resonance) techniques to better capture molecular dynamics in complex fluids, particularly in model and biological membranes, is reported. The new “full S_{c-} method”, which corrects the spectral analysis for the phase distortion effects present in the experiments, is demonstrated to enhance the sensitivity of 2D-ELDOR in reporting on molecular dynamics in complex membrane environments. That is, instead of performing spectral fitting in the magnitude mode, our new method enables simultaneous fitting of both the real and imaginary components of the S_{c-} signal. The full S_{c-} fitting not only corrects the phase distortions in the experimental data but also more accurately determines instrumental dead times. The phase corrections applied to the S_{c-} spectrum enable the extraction of the pure absorption-mode spectrum, which is characterized by much better resolution than the magnitude-mode spectrum. In the absorption mode, the variation of homogeneous broadening, which reports on the dynamics of the spin probe, can even be observed by visual inspection. This new method is illustrated with results from model membranes of dipalmitoyl-sn-glycero-phosphatidylcholine (DPPC)–cholesterol binary mixtures, as well as with results from plasma membrane vesicles of mast cells. In addition to the dynamic parameters, which provide quantitative descriptions for membranes at the molecular level, the high-resolution absorption spectra themselves may be used as a “fingerprint” to characterize membrane phases and distinguish coexisting components in biomembranes. Thus we find that 2D-ELDOR is greatly improved with the new “full S_{c-} method” especially for exploring the complexity of model and biological membranes.

© 2007 Published by Elsevier Inc.

Keywords: 2D-ELDOR; ESR; Full S_{c-} fitting; Spectral lineshape; Absorption spectrum; Plasma membrane vesicles

1. Introduction

1.1. 2D-ELDOR

Two-dimensional electron–electron double resonance (2D-ELDOR)³ techniques have in recent years been developed to study molecular dynamics in complex fluids, par-

ticularly in membrane systems. This includes studies of various systems, such as isotropic fluids [1,2], ordered fluids such as liquid crystals [3], peptides [4], polymers [5], complex fluids [6–8], model membranes [9–12], and more recently, biomembranes [13]. As a result, ESR (e.g. continuous-wave (cw)-ESR [14–18] and 2D-ELDOR techniques) has been demonstrated as a powerful tool to explore and

^{*} Corresponding author. Fax: +1 607 255 6969.

E-mail address: jhf@ccmr.cornell.edu (J.H. Freed).

¹ Present address: Department of Chemistry, National Tsing Hua University, Hsinchu, 30013, Taiwan.

² Present address: Instituto de Física de São Carlos, Departamento de Física e Informática, Universidade de São Paulo, São Carlos, Brazil.

³ *Abbreviations:* Chol, cholesterol; COSY, correlation spectroscopy; DPPC, dipalmitoyl-sn-glycero-phosphatidylcholine; DSP, dynamic spin packets; END, electron–nuclear dipolar; ESR, electron-spin resonance; FID, free induction decay; FT, Fourier transform; HB, homogeneous broadening; HE, Heisenberg spin exchange; IB, inhomogeneous broadening; IgE, Immunoglobulin E; L_d, liquid-disordered; L_o, liquid-ordered; LPSVD, linear prediction with singular-value decomposition; MOMD, microscopic order with macroscopic disorder; NLLS, non-linear least squares; PMV, plasma membrane vesicle; SECSY, spin–echo correlation spectroscopy; SF, Saxena and Freed; SLE, stochastic Liouville equation; SRLS, slowly-relaxing local structure; 2D-ELDOR, two-dimensional electron–electron double resonance; 16-PC, end-chain spin labeled phospholipid.

reveal the dynamic structure of membrane phases. For example, using spin-labeled lipids, it was shown that 2D-ELDOR displays significantly different spectra for the liquid-ordered (L_o) phase vs. the liquid-disordered (L_d) phase, and thus provides a visual distinction of these two important phases [10], since they may be related to the main components found in biomembranes. In another study [11], involving membranes of peptide dissolved in lipid, it was unequivocally shown that there are two distinctly different spectral components, respectively, representing bulk and boundary lipids which coexist [19,20].

The study of membranes has become a central theme in biophysics. Topics include phase diagrams of binary/ternary lipid mixtures, protein–lipid interactions, the molecular dynamic structures of membranes, and phase coexistence in the domains of model and biological membranes. The study of biomembranes has posed a challenge to most of the existing physical methods, including ESR. A biomembrane is complex with heterogeneous compositions, and with (dynamic) local domains. In the presence of local heterogeneity, ESR lineshapes are broadened and, consequently, the spectral resolution is reduced. From the viewpoint of data collection in time-domain experiments (e.g. 2D-ELDOR), the collected signal decays faster in the presence of heterogeneity. Thus a large part of the signal is lost during the instrumental dead-time before data collection begins. While the instrumental capabilities are continuously being improved, a method for improving spectral resolution and spectral analysis is also urgently needed to help overcome the complexity of the biological systems. This is the purpose of the present report.

2D-ELDOR techniques became a reality as a result of the development of Fourier transform (FT)-ESR experiments in the middle of 1980s [1,2,21,22]. The 2D-FT-ESR experiments include two-pulse SECSY (spin–echo correlated spectroscopy) and COSY (correlation spectroscopy) experiments, and the three-pulse 2D-ELDOR experiment, which is a Free Induction Decay (FID)-based 2D-exchange experiment [1,2,22]. 2D-ELDOR was initially found useful in reporting on the spin-relaxation mechanisms of Heisenberg spin exchange (HE) and electron–nuclear dipolar (END) interactions, in the motional narrowing regime [1–3,22]. In other applications, Bowman [23] showed how 2D-ELDOR can be used to study intermolecular chemical exchange, whereas Goldfarb and co-workers [24] demonstrated its use for slow intramolecular chemical exchange, and Dinse [25] demonstrated its potential for the investigation of transient radicals. All of these applications also involved motionally narrowed ESR spectra.

Later, as a result of continuing improvements in 2D-FT-ESR instrumentation [6,26] (e.g. achievement of short dead-times, large spectral coverage ca. 250 MHz, fast data acquisition rates) as well as the development of a comprehensive theory [6,8], it was successfully applied to the more challenging cases of complex fluids (including membranes) using nitroxide probes [6,7] wherein the molecular motions are within the slow-motional regime. In this regime, the

spectral bandwidths are large, approaching that of rigid limit spectra, inhomogeneous broadening (IB) is substantial and there is usually sufficient homogeneous broadening (HB) to yield short (homogeneous) T_2 's. The developments of the theory and computational algorithms have played an essential role in making 2D-ELDOR useful. The current 2D-ELDOR simulation program, based on the stochastic Liouville equation (SLE) [27], is performed using powerful and efficient computational methodology (based on the Lanczos algorithm) and by nonlinear least-squares fitting of the simulations to experimental spectra [8,28,29].

The 2D-ELDOR experiment is closely analogous to the 2D-exchange experiments of NMR, [1,7,8,22,30]. The 2D-ELDOR pulse sequence is illustrated in Fig. 1. It consists of three $\pi/2$ pulses. One collects the FID along t_2 (after the spectrometer dead time, t_d) for fixed values of t_1 , the preparation time and T_m , the mixing time. This process is repeated for different values of t_1 keeping T_m fixed. A double Fourier transform in t_1 and t_2 converts the signal, $S(t_1, t_2)$ into $\tilde{S}(f_1, f_2)$, which is a function of the two respective frequencies: f_1 and f_2 , as shown in Fig. 1. Actually, one collects a “hypercomplex” signal, i.e., a signal that is complex, with a real absorptive part and an imaginary dispersive part, with respect to each frequency in the 2D representation. This hypercomplex signal can be combined to give two ordinary complex signals that we call S_{c+} and S_{c-} . The former (the S_{c+} signal) is FID-like, because it is not refocused by the last or “read-out” pulse, whereas the second (the S_{c-} signal) is echolike, because it is refocused by the last pulse. These signals correspond to the coherence pathways $0 \rightarrow \mp 1 \rightarrow 0 \rightarrow -1$ for $S_{c\pm}$ as shown in Fig. 1. Other unwanted coherence pathways are canceled out by an appropriate phase cycle sequence [1,22]. In the absence of inhomogeneous broadening, the two are identical. In the presence of IB the S_{c+} and S_{c-} signals are quite different, with the S_{c-} spectra being substantially sharper due to the echolike cancellation of the IB, which does not occur for the S_{c+} spectra. In our past studies [7,9] we have found that the S_{c+} signal is much more attenuated, due to its more rapid decay during t_d , because the IB is not refocused. Thus, we make use of the strong and better resolved S_{c-} signal.

In Fig. 1(c), the so-called auto peaks are observed along the diagonal corresponding to $f_1 = f_2$. This diagonal corresponds closely to a conventional ESR spectrum (which, however is in the derivative mode unlike 2D-ELDOR) showing three hyperfine (hf) lines for a nitroxide. Peaks that are observed corresponding to $f_1 \neq f_2$ are known as the crosspeaks. These crosspeaks are a measure of magnetization transfer between hf lines by spin relaxation processes during T_m . The principal spin relaxation mechanisms for magnetization transfer are the END interactions, which lead to nuclear spin flip transitions that report on the rate of rotational reorientation, and HE with rate ω_{HE} , which reports on the bimolecular collision rate of the spin-labeled molecules. The pattern of crosspeaks enables one to distinguish the contributions from each relaxation mechanism.

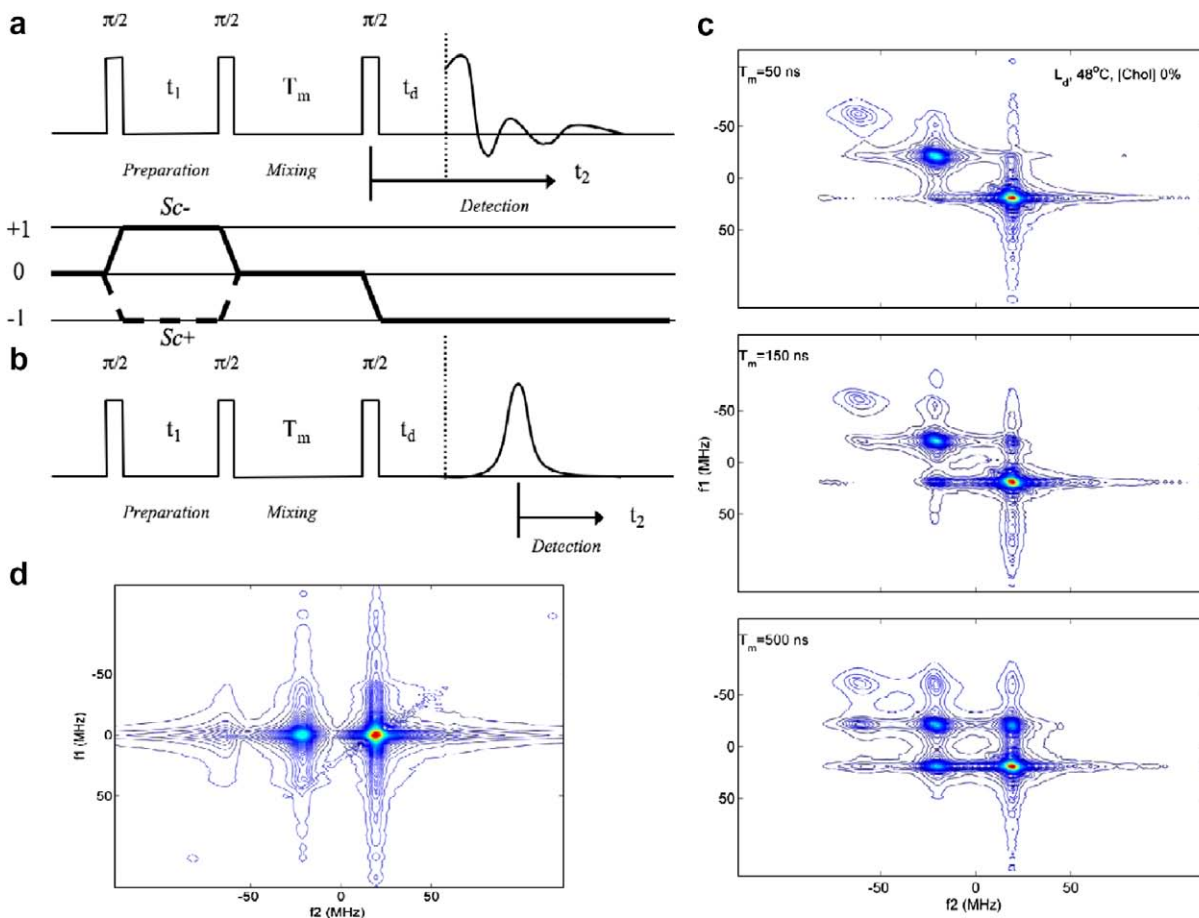


Fig. 1. The pulse sequences for (a) the standard 2D-ELDOR experiment and (b) SECSY format 2D-ELDOR experiments, (c) contour plots of magnitude 2D-ELDOR spectra vs. T_m for a model membrane (cf. Section 3.1) in its liquid disordered phase using 16PC spin label, which is an end-chain labeled phospholipid. (d) Contour plot for SECSY format for the $T_m = 50$ ns case in (c). The coherence pathways associated with the pulse sequences in (a) and (b) are also shown.

In the membrane studies used for illustration in the present work, low enough concentrations were used to keep ω_{HE} small. The 2D-ELDOR experiments are done as a series of different T_m to observe how these crosspeaks “grow-in” relative to auto peaks, as a result of these cross-relaxation mechanisms (cf. Fig. 1c). Such a series of 2D spectra vs. T_m provides, in effect, a third dimension.

IB plays an important role in the case of spectra from membrane vesicles in 2D-ELDOR. The spectra from vesicles have IB due to the Microscopic Ordering of the membrane but the Macroscopic Disorder of the sample, yielding what is referred to as MOMD spectra. It is possible to utilize the different shapes of the auto peaks and crosspeaks to distinguish the contribution to IB from proton super hyperfine (shf) interactions, which is the same for each hf line, and the MOMD effect, which varies for each hf line. As we noted, for the S_{c-} 2D-ELDOR spectra, there is a partial suppression of IB of the auto peaks due to their echo-like properties. However, since the IB due to MOMD is different for the different hf lines, and the crosspeaks result from magnetization transfer between different hf lines, then the echo-like cancellation is less effective for these peaks. Therefore, the crosspeak shapes, compared

with the auto peak shapes, provide a sensitive measure of the MOMD inhomogeneity effects and hence the extent of ordering. The effect of MOMD can be discerned even in the shapes of the auto peaks (cf. Fig. 1c). Along the $f_1 = f_2$ diagonal, one observes the full IB, comparable to a cw-ESR experiment. However, in the perpendicular direction, the widths are reduced by the echo-like cancellation effect discussed above.

There is a variant of the 2D-ELDOR experiment of Fig. 1(a), which leads to the HB being clearly displayed along one spectral dimension (i.e. f_1), whereas the auto peaks and their IB appear along the other (i.e. f_2) spectral dimension, (cf. Fig. 1d). This may be achieved by the modification shown in Fig. 1(b), which emphasizes the detection of the echo decay. The case of Fig. 1(a) is referred to as the ELDOR mode, whereas that of Fig. 1(b) as the SECSY mode (for spin-echo correlation spectroscopy). It has been shown theoretically [8,31] that: an experiment performed in the ELDOR mode may be translated into the SECSY mode simply by letting t_2 in the former be replaced by $t_1 + t_2$ (thus redefining t_2) in the processing of the data, as is suggested by Fig. 1(a) and (b), and then performing a Fourier transform (FT) with respect to t_1 and the redefined

t_2 . This is known as a shearing transformation. Furthermore, the homogeneous linewidths are indeed displayed along f_1 . This clear separation of IB and HB of the auto peaks is extremely valuable in analyzing 2D-ELDOR spectra, especially for cases where crosspeak development is very weak. We will have occasion to benefit from this SECSY mode in the present study, with a number of examples (using the shearing transformation) shown below.

1.2. Phase corrections and the pure absorption mode

Whereas, the 2D-ELDOR experiment is a hypercomplex one, with real and imaginary components of the signal with respect to both frequencies, f_1 and f_2 , the maximum resolution would be obtained by extracting the pure absorption mode, as is commonly done in 2D-NMR. However, this has proved to be challenging in 2D-FT-ESR. In the case of well-resolved, homogeneous spectral lines, as may be encountered in motionally narrowed spectra, a method of Linear Prediction with Singular Value Decomposition [32] (LPSVD) enables the recovery of the full-absorption from the experimental hypercomplex data. In the opposite limit of very slow motions and/or dominance of the spectral lineshape by the IB, Saxena and Freed (SF) provided a method from recovery of the 2D absorption spectrum [33]. That method recognizes the fact that in such circumstances only the S_{c-} part of the full hypercomplex spectrum is available. (We have already discussed that the S_{c+} part of the 2D spectrum, is found to decay rapidly in the presence of IB. Thus, unlike in NMR, it is not useful for further data analysis). Thus, the natural representation of the data is the SECSY-mode representation, since the S_{c-} signal is equivalent to detection of the spin-echo. The SF method then seeks the best estimate of a single set of phase corrections to apply to the inhomogeneously broadened 2D-ELDOR data in the SECSY mode. This is indeed a valid approach in the limit in which the IB spectrum is composed of many dynamic spin packets (DSP), which cover a quasi-continuum across the largely IB spectrum.

We found, however, that the MOMD-type 2D-ELDOR spectra obtained from spin-labeled lipids in membranes are in an intermediate regime, wherein HB and IB are of comparable magnitude. This, on the one hand, prevented the use of the LPSVD method, which assumes simple Lorentzian lines (e.g. negligible IB), and on the other hand prevented the use of the SF method, which implicitly assumes that the IB predominates, so the phase correction, linear in f_2 , is applied uniformly across the spectrum. The rigorous requirement, however, is that the linear phase correction be applied to the characteristic resonant frequency for each dynamic spin-packet, (which can be obtained by diagonalizing the stochastic-Liouville operator). For example, in the motional narrowing limit of distinct HB lines, the phase of each hyperfine line is automatically corrected in the LPSVD method according to its own characteristic frequency. Also, in the limit of very slow motions, the application of the linear phase correction across the IB

spectrum is consistent with the quasi-continuum of dynamic spin packets, i.e. an infinitesimal displacement in frequency moves from one to the next DSP. However, these two limiting cases are incompatible, e.g. for a single broad but HB line, it would be incorrect to apply the linear phase correction (e.g. $a_2 f_2$) at each point in the spectrum; instead one must just apply it to the central resonant frequency of the line as is done in the LPSVD method. Thus when HB and IB are comparable, a different approach is required than either of the two limiting approaches.

The approach we have adopted is to determine the phase corrections as an integral part of the NLLS fitting procedure. To this purpose the standard 2D-ELDOR simulation and fitting routines have been modified to include fitting these phase corrections. This is a relatively simple addition to the programs, which already include the optimization of spectral scaling factors, etc. This enables one to use the optimized phase corrections properly for each DSP obtained from the diagonalization of the SLE, during the course of the NLLS fitting procedure.

The most important benefit of this procedure is that the S_{c-} signals (in the SECSY format) are utilized in their full complex format, i.e. both the real and imaginary parts of the S_{c-} data are used simultaneously in the fitting. This replaces the past use of fitting just the magnitude of the S_{c-} signal, with its inherent loss of resolution. The full S_{c-} signal preserves the resolution inherent in the pure absorption signal.

Once the best fit is obtained to the full S_{c-} signal, it is a simple matter to recover the pure absorption S_{c-} signal (in the SECSY mode) from the theoretical fit. Even though the fit provides the phase corrections, it is a less trivial matter to process the experimental S_{c-} signal to return the experimental pure absorption, for the reasons discussed above. That is, the experimental data are not directly decomposable into the various DSP. Therefore, we have utilized an approximate approach that we also describe.

In summary, in this report we present the full S_{c-} method. In addition, we illustrate how it improves 2D-ELDOR techniques for characterizing the molecular dynamic structures of complex fluids, including biomembranes.

2. Theoretical aspects

2.1. 2D-ELDOR

The three- $\pi/2$ -pulse sequence of the 2D-ELDOR experiment is illustrated in Fig. 1(a) and its SECSY format is shown in Fig. 1(b), and they have been described in Section 1.1. Note that the common procedure is to perform the standard 2D-ELDOR experiment of Fig. 1(a) and then use the shearing transformation to obtain the SECSY format. This is the perspective we therefore use in the theoretical description in this section. The 2D-ELDOR signal is in a “hypercomplex” format as noted in Section 1. In the actual experiment we measure this signal as two distinct

complex signals S' and S'' [8,33]. These two signals can then be combined to give two complex signals that we call S_{c+} and S_{c-} which are given by Eq. (1). These $S_{c\pm}$ signals are associated with the distinct coherence pathways shown in Fig. 1.

$$S_{c\pm}(t_1, T_m, t_2) = S'(t_1, T_m, t_2) \pm i \cdot S''(t_1, T_m, t_2) \quad (1)$$

The time-domain 2D-ELDOR $S_{c\pm}$ signals can be written formally as [6,8]

$$S_{c\pm} = \langle v_{-1} | O_{-1} e^{-A_{-1} t_2} O_{-1}^{\text{tr}} P_{(-1 \rightarrow 0)} O_0 e^{-A_0 T_m} O_0^{\text{tr}} P_{(0 \rightarrow \mp 1)} O_{\mp 1} e^{-A_{\mp 1} t_1} O_{\mp 1}^{\text{tr}} | v_{\mp 1} \rangle \quad (2)$$

where \mathbf{P} represents the pulse propagator superoperator, and the \mathbf{O} and \mathbf{A} matrices are, respectively, the (complex) orthogonal transformation matrix, which is composed of the eigenvectors, and the diagonal matrix of complex eigenvalues, of the stochastic Liouville operator \mathcal{L} (i.e. $\mathbf{O}_j^{\text{tr}} \mathcal{L}_j \mathbf{O}_j = \mathbf{A}_j$) contained in the SLE which describes the time evolution of the electron-spin bearing molecules in both spin space and molecular orientational space [8,27–29]; the subscripts indicate the order of the coherence. The vectors $|v_{\mp 1}\rangle$ and $\langle v_{-1}|$ are the right and left hand vectors representing the effects of the first excitation pulse and the signal detection, respectively. (Note that $O_{+1} = O_{-1}^*$, $\langle v_{-1}|^{\text{tr}} = |v_{-1}\rangle$, $|v_{+1}\rangle = |v_{-1}\rangle^*$, and $A_{-1} = A_{+1}^*$ cf. [8]).

The differences between the S_{c+} and S_{c-} signals are found to depend on the motional rates as well as the MOMD effect, and on the other sources of IB (e.g. unresolved superhyperfine interactions with protons), which are not explicitly included in the SLE, and are taken to be Gaussian. It is convenient to first illustrate the features of these signals for the simpler special case of $T_m = 0$. Then Eq. (2) can be written as [8]

$$S_{c+} = \sum_i w_i^2 e^{-\lambda_i(t_1+t_2)} \times e^{-\Delta(t_2+t_1)^2} \quad (3a)$$

$$S_{c-} = \sum_{i,j} w_i e^{-\lambda_i t_2} (O_{-1}^{\text{tr}} O_{-1}^*)_{i,j} e^{-\lambda_j^* t_1} w_j^* \times e^{-\Delta(t_2-t_1)^2} \quad (3b)$$

where i and j refer to the eigenmodes with (complex) eigenvalues λ_i and λ_j , respectively; [note $\lambda_j \equiv (A_{-1})_{jj}$]. These eigenmodes are what we have referred to in Section 1 as the dynamic spin packets (DSP). Also, w_i is the scalar product of the i th eigenvector (representing the i th eigenmode) with the right hand vector, and Δ is the additional Gaussian IB. The two equations become nearly equivalent in the fast-motional regime, (i.e. for rotational rates, $R > 10^8 \text{ s}^{-1}$) because the $O_{\mp 1}$ become real, so $O_{-1}^* = O_{-1}$ and $(O_{-1}^{\text{tr}} O_{-1}^*) = \delta_{i,j}$. However, the S_{c-} signal shows an echo-like cancellation of the Gaussian and other IB, whereas the S_{c+} signal does not. As the motion slows sufficiently, the S_{c+} and S_{c-} signals are no longer equivalent, even if $\Delta = 0$ (and if there is no MOMD effect). There are two factors that affect the evolution of the signal decays differently: (i) in the slow-motional regime, the elements of $O_{\mp 1}$ take on complex values so $(O_{-1}^{\text{tr}} O_{-1}^*) \neq \delta_{i,j}$ and the S_{c-} signal loses its coherence as a result of interferences between

eigenmodes, whereas the S_{c+} maintains its coherence (cf. Eqs. (3)); (ii) the increased IB, due to the decreased molecular motion (as well as the MOMD effect and the unresolved proton superhyperfine structure), becomes a dominant factor in the signal decay, such that the S_{c+} and S_{c-} decay, respectively, with the inhomogeneous T_2^* and homogeneous T_2 along the $t_1 = t_2$ axis (cf. Eqs. (3)), where $T_2 \gg T_2^*$. That is, along the $t_1 = t_2$ axis (most of) the IB is cancelled out in the S_{c-} signal. Clearly the Gaussian IB represented by Δ is cancelled. One should note that each complex eigenvalue may be expressed as $\lambda_j = T_{2,j}^{-1} + i\omega_j$, where the imaginary part represents the resonant frequency of the j th “dynamic spin packet”. This frequency term is also cancelled for $t_1 = t_2$ for the $i = j$ terms in the double sum of Eq. (3b). Thus the S_{c-} signal decays primarily with just the $T_{2,j}$. This accounts for the echo-like refocusing property of the S_{c-} signal. The S_{c+} signal decays more rapidly with T_2^* , and therefore, is often found to be much weaker than the S_{c-} signal for finite dead times. The S_{c-} signal has thus been the main focus in ESR data analysis, (while both S_{c-} and S_{c+} signals are useful in NMR).

We now return to the 2D-ELDOR signal, when $T_m > 0$ in Eq. (2) and focus on the S_{c-} signal. The time-domain S_{c-} signals in the standard and SECSY formats are, respectively, shown in Eqs. (4) and (5),

$$S_{c-}^{\text{ELDOR}}(t_1, T_m, t_2) \propto \sum_{nkj} K_{nkj} \exp[-\lambda_j^* t_1] \exp[-(A_0)_k T_m] \times \exp[-\lambda_n t_2] \exp\{-\Delta(t_2 - t_1)^2\} \quad (4)$$

$$S_{c-}^{\text{SECSY}}(t_1, T_m, t_2) \propto \sum_{nkj} K_{nkj} \exp[-(\lambda_j^* + \lambda_n)(t_1)] \times \exp[-(A_0)_k T_m] \exp[-\lambda_n t_2] \exp\{-\Delta t_2^2\} \quad (5)$$

where K_{nkj} are complex coupling coefficients which may be obtained from a comparison with Eq. (2). The utility of the SECSY format follows from Eq. (5). There is a cancellation of the frequency term: $\lambda_j^* + \lambda_n$ in t_1 . (Strictly speaking this cancellation is exact for the $n = j$ terms in the sum, but in practice it remains a good approximation for the autopeaks where (i) $\omega_n \approx \omega_j$ and (ii) interference terms for which $n \neq j$ are generally relatively small.) This means that the signal decays with $T_{2,j}$ along the t_1 axis, and after Fourier transformation just the HB shows up along ω_1 . In addition, the IB linewidth, i.e. the last term of Eq. (5), as well as the frequency term in λ_j , appears in the signal along the ω_2 direction. This clear separation of HB from IB along the autopeaks is of great value in analyzing 2D-ELDOR spectra in the SECSY format as discussed in Section 1. However, in the presence of experimental artifacts (e.g. the existence of dead-times and imperfect spectral coverage by the pulse) the separation of HB from IB in the SECSY format is significantly hampered. However, this separation is made possible when the SECSY spectra are displayed in the pure absorption mode [33]. To convert experimental data to the pure absorption mode, phase corrections must be performed prior to the spectral conversion. We discuss

the conversion of experimental data to the pure absorption mode in the following sections.

2.2. The full S_{c-} method

2D-ELDOR spectra have, in the past, been presented in the magnitude mode, i.e. the absolute amplitude of the complex S_{c-} signals in the frequency domain. It is helpful to present the 2D-ELDOR spectrum in the magnitude mode because the phase distortions caused during experiments are cancelled in such a format. However, the spectral resolution is sacrificed in the magnitude mode because it is composed of mixtures of the absorptive and dispersive signals. To separate the absorptive part of the signal from the experimental data, it is necessary to first obtain the information about the needed phase corrections. The “full S_{c-} method” that we present in the present report is a reliable way of determining the phase corrections from the experimental data.

We introduce the phase corrections in Eq. (6) for the signals, S' and S'' , that we actually measure in real 2D-ELDOR experiments, [1,8,33], (cf. above):

$$S'(t_1, T_m, t_2) = \frac{1}{2} \sum_{lkn} C_{lkn} \exp[-(A_0)_k T_m] \\ \times \exp[-\lambda_n(t_2 + b_2) - i \cdot a_2] \\ \times \sum_j \left[\begin{array}{l} \exp\{-\Delta(t_2 + t_1)^2\} \times B_{ij}^+ \exp[-\lambda_j(t_1 + b_1)] \\ + \exp\{-\Delta(t_2 - t_1)^2\} \times B_{ij}^- \exp[-\lambda_j^*(t_1 + b_1)] \end{array} \right] \quad (6)$$

$$S''(t_1, T_m, t_2) = \frac{1}{2i} \sum_{lkn} C_{lkn} \exp[-(A_0)_k T_m] \\ \times \exp[-\lambda_n(t_2 + b_2) - i \cdot a_2] \\ \times \sum_j \left[\begin{array}{l} \exp\{-\Delta(t_2 + t_1)^2\} \times B_{ij}^+ \exp[-\lambda_j(t_1 + b_1)] \\ - \exp\{-\Delta(t_2 - t_1)^2\} \times B_{ij}^- \exp[-\lambda_j^*(t_1 + b_1)] \end{array} \right]$$

Here $\sum_{\epsilon} C_{lkn} B_{ij}^- = K_{nkj}$ and $B_{ij}^+ = (B_{ij}^-)^*$ and are further defined in Ref. [33]. In Eq. (6) the coefficients, b_1 , b_2 , and a_2 , are the linear phase correction terms, which are needed in the theoretical expression in order to correspond to actual experiments (i.e. to include the effects of such artifacts as imperfect pulse shape, imperfect bandwidth coverage, and finite dead-times). The time-domain equation of the ELDOR signals in Eq. (4) can be re-written using Eqs. (1) and (6) with inclusion of these phase factors,

$$S_{c-}^{\text{ELDOR}}(t_1, T_m, t_2) \propto \sum_{nkj} K_{nkj} \exp[-\lambda_j^*(t_1 + b_1)] \\ \exp[-(A_0)_k T_m] \times \exp[-\lambda_n(t_2 + b_2) \\ - i \cdot a_2] \exp\{-\Delta(t_2 - t_1)^2\} \quad (7)$$

Upon applying the shearing transformation, i.e. $t_2 \rightarrow t_1 + t_2$, Eq. (7) becomes:

$$S_{c-}^{\text{SECSY}}(t_1, T_m, t_2) \propto \sum_{nkj} K_{nkj} \exp[-(\lambda_j^* + \lambda_n)(t_1 + b_1)] \\ \times \exp[-(A_0)_k T_m] \exp[-\lambda_n(t_2 + \delta b) \\ - i a_2] \exp\{-\Delta t_2^2\} \quad (8)$$

where the phase factor $\delta b = b_2 - b_1$ is determined from the difference of the two correction factors b_1 and b_2 . (Saxena and Freed [33] used a slightly different notation in their form of Eq. (8). They did not utilize Eq. (7), although we do in the full S_{c-} method. Our notation for the phase corrections maintains consistency between Eqs. (7) and (8), and it allows one to process the theoretical simulations in exactly the same manner that we process our experimental data, i.e. from Eqs. (5)–(7) and then (8).) The phase distortions contributed from the phase factors in Eqs. (7) and (8) are cancelled in the traditional magnitude mode, but are observable when displaying the S_{c-} signal in its real and imaginary formats.

Fig. 2(a) and (b) shows, respectively, 2D-ELDOR experimental and simulated spectra in the full S_{c-} domain. In the magnitude mode (not shown), which is the absolute amplitude of the real and imaginary parts, the simulated spectrum agrees very well with the experimental spectrum. But, because of the phase distortions in the real experiment, the simulated spectrum is distinctly different in the full S_{c-} domain without correcting for phase distortions. We now describe how we reliably obtain phase correction factors directly from the (distorted) real and imaginary parts of the raw data. The idea is simply to simultaneously fit a spectrum in the full S_{c-} domain to obtain the set of phase factors (cf. b_1 , b_2 , and a_2 in Eqs. (7) and (8)) as part of the fitting process. Also, we have found it preferable to simultaneously fit the data in the normal ELDOR (Eq. (7)) and SECSY formats (Eq. (8)), to obtain better consistency. We remind the reader that the experiments are all collected in the normal ELDOR mode, and the SECSY formats are obtained from the same data set by employing the shearing transformation. The theoretical simulations are processed in exactly the same way. The overall fitting procedure is best accomplished by first fitting the spectra in the magnitude mode and then using the dynamic and ordering parameters, that are found, as seed values for initiating the full S_{c-} method.

The procedure for performing the full S_{c-} method is summarized in the following.

- (i) Perform the spectral fitting simultaneously in both the ELDOR and SECSY formats (with comparable weighting) in the magnitude mode using the 2D NLLS (nonlinear least squares) program [29], where both experimental and theoretical spectra are processed in an identical manner, (i.e. Eqs. (1) and (6) yielding Eq. (7), then Eq. (8); after which the magnitude modes of Eqs. (7) and (8) are taken).
- (ii) Then, use the best-fit dynamic parameters obtained in the magnitude-mode fits (i.e. step i) as seed values and repeat the spectral fitting for both the ELDOR and SECSY formats in the full S_{c-} domain. In most cases, the simulated spectra in the full S_{c-} domain are distinctly different from the experimental spectra, even though good quality fits have been achieved for the magnitude-mode. This, in large part, is because the

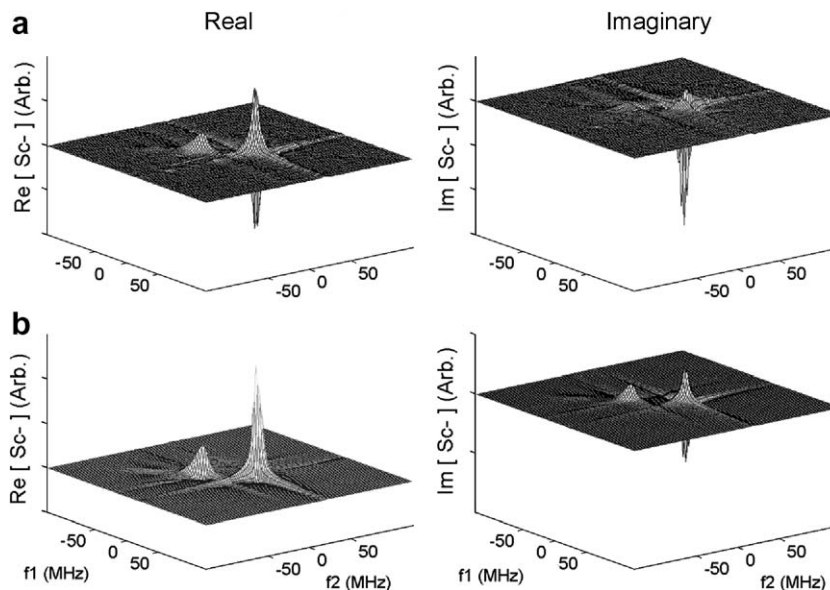


Fig. 2. Spectra ($T_m = 50$ ns) displayed in the full S_{c-} domain: (a) experimental results with their inherent phase distortions, and (b) the simulated spectrum without any phase adjustments. The experimental spectra (cf. ref. 13) are from plasma membrane vesicles at 15 °C, which have been stimulated by antigen of IgE receptors, and which contain the spin-label 16PC, (cf. Section 3.2).

phase corrections have not yet been made. We suggest that the phase factors should be fit prior to varying the dynamic parameters (from their seed values) in this step. The large spectral differences due to the phase distortions, as shown in Fig. 2(a) vs. (b), can be corrected by the three phase correction factors.

- (iii) Then all fitting parameters may be varied to obtain the final results. We find that the better resolved and more extensive data set, (i.e. the real and imaginary parts of S_{c-}), yield more accurate dynamic parameters, even though the phase correction factors are also included in the fits. In general, we find that the optimum phase factors are close to the values obtained in step (ii). Also, in most cases the (more accurate) values of the dynamic parameters are close to those obtained from the magnitude fits.

It is important to note that in all three steps (i, ii, and iii) a set of 2D-ELDOR spectra for several mixing times, T_m are simultaneously fit [3,6–11]. In the full S_{c-} method, this set of spectra vs. T_m are fit to the same phase corrections, since all the experimental settings are kept constant, except for T_m .

We show in Fig. 3 a comparison of an experimental result and the best fit obtained by the full S_{c-} method in both the ELDOR (Fig. 3a) and SECSY (Fig. 3b) modes. The spectra are shown as contour plots. One sees that in the ELDOR mode the spectral fits are very good. In the SECSY mode the fits are not quite as good. We find that the SECSY mode, which more effectively separates the HB from the IB, is more discriminating in the fits. Our experience in fitting extensive experiments [12,13] by the full S_{c-} method using the MOMD theoretical model leads us to conclude that Fig. 3(b) represents a good fit for the

SECSY mode. One may, in the future, wish to analyze spectra of such good resolution by improved models, such as the slowly-relaxing local structure (SRLS) model [34,35]. (However, we do wish to note that by weighting the SECSY spectra more heavily in the NLLS fitting relative to the standard ELDOR spectra, then the agreement between the experimental and theoretical SECSY mode spectra can be improved somewhat.)

We find that the phase correction factors fall into the following ranges: b_1 and $b_2 \sim 1.5$ – 5.5 ns, and $a_2 \sim -0.5$ to -2 radians. The b_1 and b_2 may be regarded as small corrections to the dead-times in t_1 and t_2 which range in our experiments from ~ 25 to ~ 35 ns. These dead-times are measured from the end of the pulse to the beginning of the data acquisition. But, since the pulse shape is not a perfect square hard pulse and is of finite duration, this correction is needed in both the t_1 and t_2 domains.

2.3. Pure absorption lineshapes

In addition to improving the accuracy of fitting to experiment, these phase factors also enable one to recover an approximate pure absorption spectrum directly from the experimental data. But first we consider the rigorous pure absorption lineshapes that are readily obtained from the simulations. They enable a useful way of displaying the best-fit spectrum. They are obtained exactly as described by Saxena and Freed [33], (who however only utilize the SECSY mode and focus just on the auto-peaks, cf. below). That is one may use either Eq. (7) or (8) followed by a double Fourier transform, where the real part is taken at each step as summarized in Eq. (9).

$$S_{c-}(\omega_1, T_m, \omega_2) = \Re[\mathbf{FT}_{t_2}\{\Re[\mathbf{FT}_{t_1}\{S_{c-}(t_1, T_m, t_2)\}]\}] \quad (9)$$

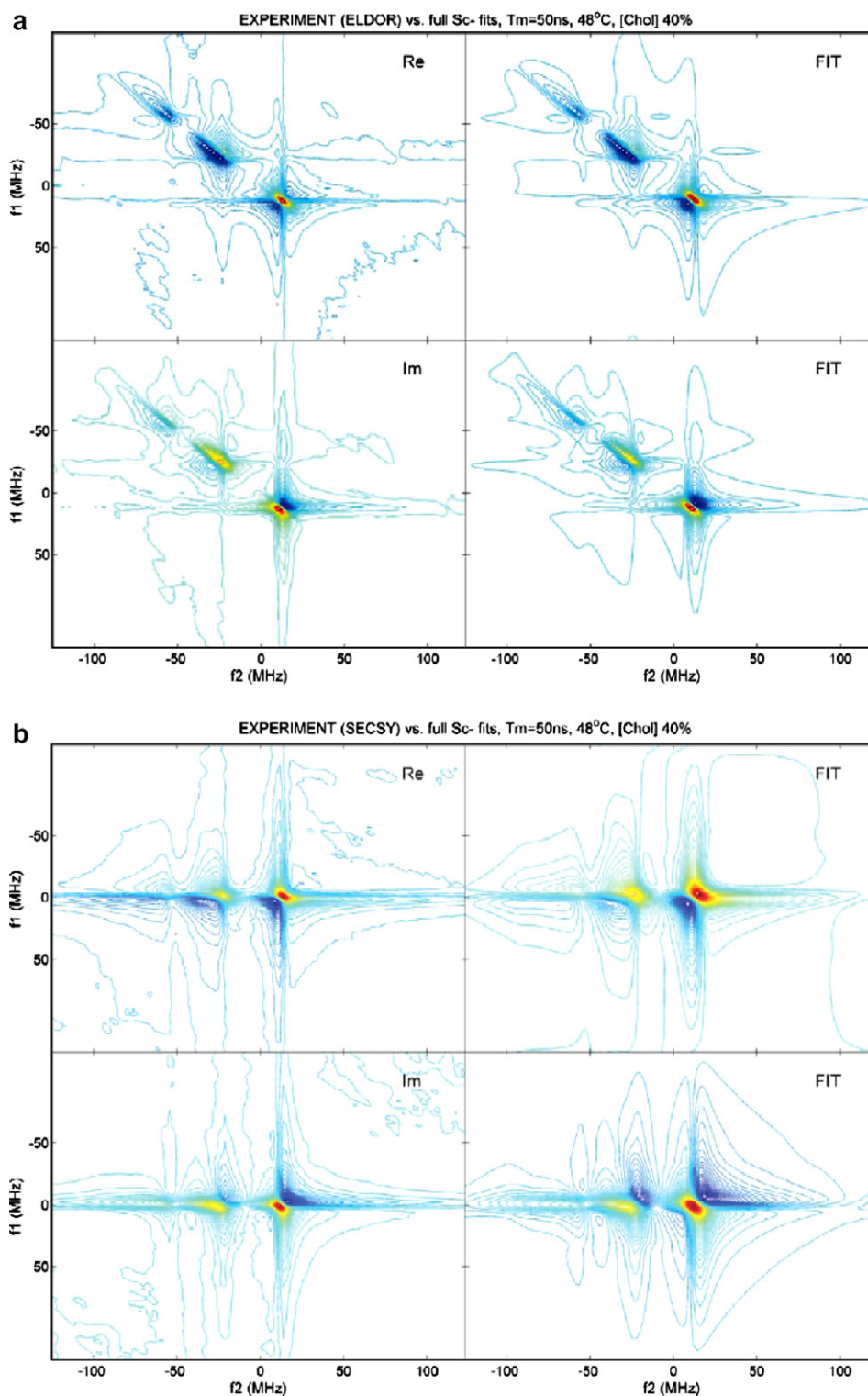


Fig. 3. 2D-ELDOR spectrum, shown as contours ($T_m = 50$ ns), of 16PC in a model membrane composed of 60% of the phospholipid DPPC and 40% cholesterol at 48°C in the liquid-ordered phase (cf. Section 3.1). The spectra are shown in the full S_{c-} display with the real signal in the upper part and the imaginary signal in the lower part. The plots contain positive and negative values in intensity. The color map varies from red, (which corresponds to the largest positive value) to yellow, light blue (zero), and dark blue (which corresponds to the smallest negative value).⁴ The experimental result is shown on the left side, with the best fit to a MOMD model shown on the right side. Fig. 3(a) displays the spectrum in the ELDOR mode, whereas Fig. 4(b) shows the SECSY mode. (The fits correspond to the parameters for Fig. 5 below.) (For interpretation of the references to color in this figure legend, the reader is referred to the web version of this paper.)

where $S_{c-}(t_1, T_m, t_2)$ on the right hand side can either be S_{c-}^{ELDOR} or S_{c-}^{SECSY} . In this procedure one can set $b_1 = b_2 = a_2 = 0$ in Eqs. (7) and (8). This produces the pure absorption for $t_d = 0$, which can be of theoretical interest. However, as SF[33] have shown, the effects of the finite dead-time, which suppress rapidly decaying eigenmodes, may be introduced by setting t_1 and t_2 after the respective dead-times and by setting $b_1 = t_{1d}$, $b_2 = t_{2d}$, and $a_2 = 0$. This enables a better comparison with the experimental approximate pure absorption spectra.

In principle, the experimental data could be directly processed to yield the pure absorption according to Eq. (9). However the data must be phase corrected, as rigorously expressed by Eqs. (7) and (8). But this is not possible in most cases, because the experimental data are not directly resolvable into the eigenmodes as needed in Eqs. (7) and (8). (One exception is for well-separated and homogeneously broadened motionally-narrowed lines). Instead we obtain an approximate pure absorption from the experimental data in the SECSY format by the SF procedure [33] given by Eq. (10).

$$\begin{aligned}
 S_{c-}^{\text{SECSY}}(t_1, T_m, t_2) &\xrightarrow{\text{FT}_2} S_{c-}^{\text{SECSY}}(t_1, T_m, \omega_2) \\
 &\xrightarrow{\text{phase correction}} \begin{bmatrix} \cos \phi_2 \cdot \Re[S_{c-}^{\text{SECSY}}(t_1, T_m, \omega_2)] \\ -\sin \phi_2 \cdot \Im[S_{c-}^{\text{SECSY}}(t_1, T_m, \omega_2)] \end{bmatrix} \\
 &\equiv S_{a-}(t_1, T_m, \omega_2) \\
 &\xrightarrow{\text{FT}_1} S_{a-}^{\text{SECSY}}(\omega_1, T_m, \omega_2) \\
 &\xrightarrow{\text{phase correction}} \begin{bmatrix} \cos \phi_1 \cdot \Re[S_{a-}(\omega_1, T_m, \omega_2)] \\ +\sin \phi_1 \cdot \Im[S_{a-}(\omega_1, T_m, \omega_2)] \end{bmatrix} \\
 &\equiv S_{a-}^{\text{abs}}(\omega_1, T_m, \omega_2) \quad (10)
 \end{aligned}$$

where

$$\phi_1 = b_1 \omega_1, \quad \phi_2 = a_2 + \delta b \omega_2 \quad (10a)$$

Eq. (10) expresses the fact that the phase corrections are introduced directly to the experimental data in the frequency domain: that is ϕ_2 is utilized first after a single FT with respect to t_2 , and then ϕ_1 , is utilized after a second FT, with respect to t_1 . This procedure implicitly assumes that the experimental spectra are a continuum of DSP. This becomes the rigorously correct result in the limit when the (slow-motional) spectra are dominated by inhomogeneous broadening. Otherwise, it is still a useful representation of the experimental results, in which the very good resolution of a pure absorption spectrum is obtained. At any rate, the actual data fitting by the full S_{c-} method is itself rigorously valid over the whole motional regime.

An experimental 2D-ELDOR spectrum in the SECSY mode obtained from a plasma-membrane vesicle (PMV) sample containing the end-chain spin-labeled phospholipid, 16-PC is plotted in Fig. 4(a) and (b), respectively, representing the real and imaginary parts of the S_{c-} sig-

nals. Due to phase distortion effects mentioned above, the in-phase and quadrature components of the S_{c-} signals are mixtures of absorptive and dispersive spectra. We recover the approximate pure absorption-mode spectrum according to Eq. (10), as shown in Fig. 4(d). The narrow, largely homogeneous absorptive lineshapes along f_1 (Fig. 4d) and the IB along f_2 may be compared with the broader magnitude spectrum in Fig. 4(c). The contour plots for the spectra in the magnitude mode and the absorption mode are also displayed in Fig. 4 to further emphasize the improved spectral resolution provided by the recovered absorption spectrum. The spectrum in Fig. 4(d) has some weak non-positive cross-peaks (not shown). This is one of only a few cases in our studies that show non-positive values in the cross-peaks. Although the cross-peaks in recovered absorption spectra are not necessarily positive [33], we found in our studies that most of the recovered absorption spectra are all positive in both auto- and cross-peaks.

2.4. Comparison with the Saxena–Freed method

The method of Saxena and Freed is based on utilizing the experimental 2D-ELDOR signal in the SECSY mode. They argue that to a good approximation the signal from the auto-peaks in the pure absorption must be positive. They then optimize the phase factors discussed above by minimizing the negative excursions in the absorption spectrum, as defined by Eq. (10), but just for the auto-peaks. A drawback of this method is that the numerical minimization may become stuck in local minima and/or return several possible sets of solutions for the phase factors, as we have found. Furthermore, different sets of phase factors obtained in the SF method can satisfy the criterion of rendering a positive absorption, but not necessarily fit well to the full S_{c-} spectrum, which includes both the real and imaginary parts, as well as all auto and cross-peaks. In addition, as we have discussed above, Eq. (10) is rigorously correct only in limiting cases, which further interferes with the SF method.

The full S_{c-} method overcomes both weaknesses of the SF method. It significantly reduces the ambiguity of the fitting parameters and unambiguously extracts the phase factors in fitting the data, as we have found. Also, it is based on the rigorous theory expressed by Eqs. (7) and (8). Indeed the application of Eqs. (7) and (8) presumes that a good theoretical model for the dynamics is being used. But this is not a new requirement for the extraction of useful information from the 2D-ELDOR spectrum. One needs an appropriate theoretical model to analyze even the spectrum in the magnitude mode, where phase factors are irrelevant. We do find that in the non-linear least squares fitting the phase factors are not very substantially correlated with the dynamic and ordering parameters, so finer aspects in modeling the dynamics are not likely to significantly affect the estimation of the phase factors.

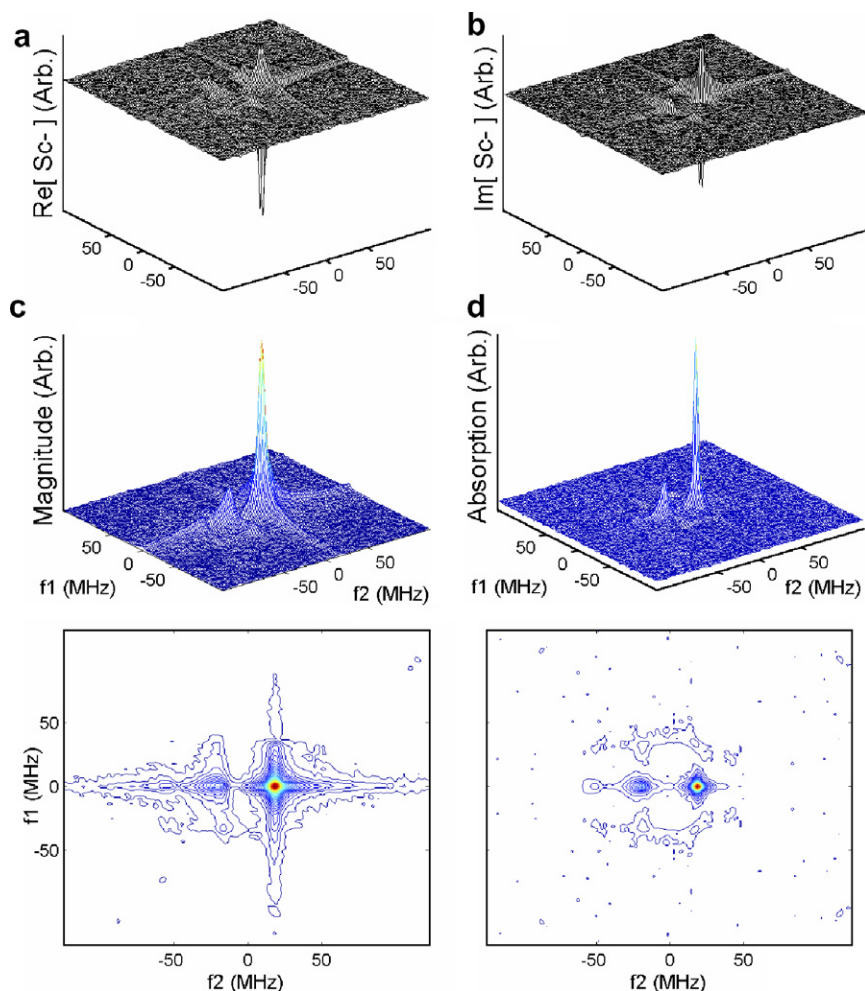


Fig. 4. 2D-ELDOR spectra ($T_m = 400$ ns) of 16PC in unstimulated PMV at 30 °C (cf. Section 3.2) displayed in the full S_{c-} domain, respectively, (a) the real and (b) the imaginary parts of the S_{c-} signal in the SECSY format.⁴ The motivation of obtaining the pure absorption spectrum is clearly demonstrated by comparing (c) the magnitude-mode spectrum with (d) the absorption-mode spectrum, where the latter shows much better spectral resolution.

3. Applications of the full S_{c-} method

The full S_{c-} method has been applied to study the dynamic molecular structures of model [12] and biological membranes [13]. In this section we utilize some of these results to focus on the advantages provided by the full S_{c-} method.

3.1. Model membrane study: binary mixtures of DPPC–cholesterol

We have studied the model (multilamellar vesicle) membrane system of dipalmitoyl-sn-glycero-phosphatidylcholine (DPPC)–cholesterol (Chol) binary mixtures using 2D-ELDOR techniques [12]. We initially performed the spectral fitting in the traditional magnitude mode, and we found that the spectral fits were not very satisfactorily obtained especially at lower temperatures. One problem is that the spectral lineshapes at lower temperatures are dominated by IB in the regime of slow motions and high

ordering, and therefore, the spectral resolution is reduced. Another problem is that two phases can coexist, so there is more than one component in the spectrum. Both features make it difficult to analyze, given the limited resolution of the magnitude spectra, as was previously pointed out [10].

The full S_{c-} method has now been employed to study this model membrane system [12]. Good fits were successfully and unambiguously obtained in all cases in both the ELDOR and SECSY formats. One such example is shown in Fig. 3.⁴ Fig. 5 shows 2D-ELDOR spectra from 16PC in the DPPC-Chol binary lipid system in the SECSY format.⁴ It is for results in the liquid-ordered (L_o) membrane phase.

⁴ Experiments were performed at Ku band (17.3 GHz). Three 4 ns $\pi/2$ pulses were used in the experiments. The time, t_1 between the first two pulses, was stepped out with 128 steps of 2 ns each. Each FID was collected along t_2 with a step size of 1 ns for a total of 256 ns. Typical dead times were ~ 35 ns for t_1 and $28 \sim 37$ ns for t_1 and t_2 , respectively. A 32-step phase cycle sequence [9] was used to form the hypercomplex 2D-ELDOR signal.

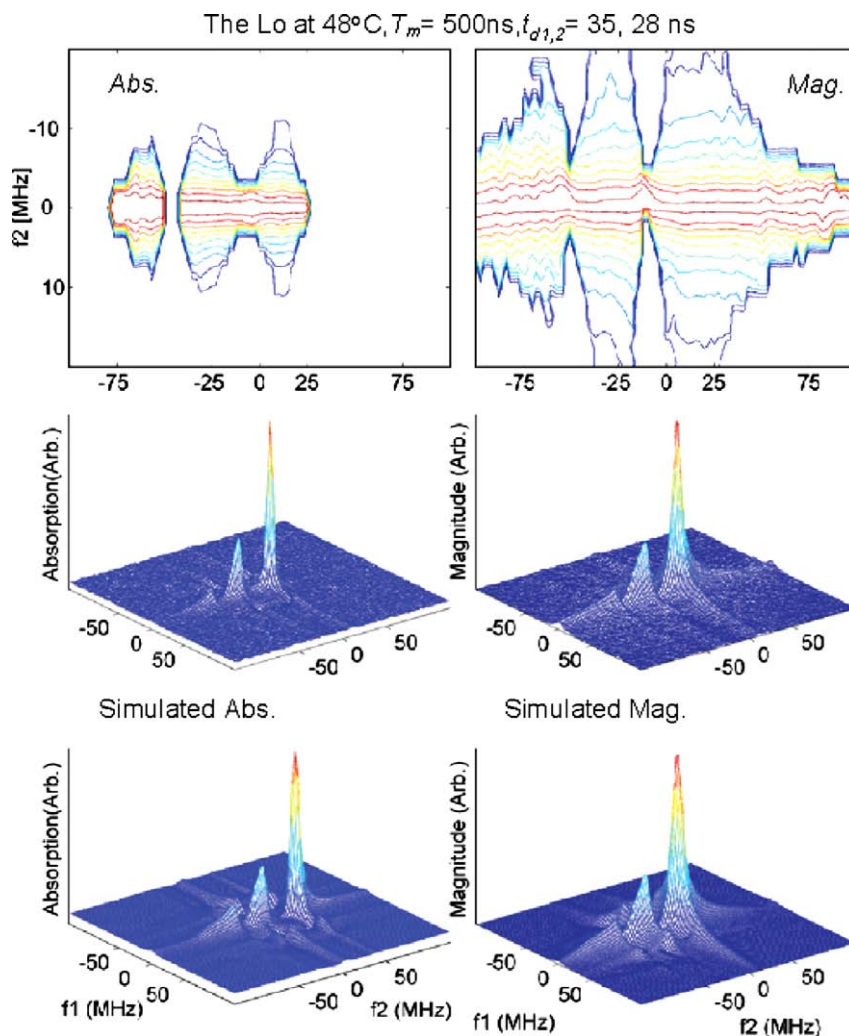


Fig. 5. The 2D-ELDOR spectra ($T_m = 500$ ns) in the SECSY format for 16PC in DPPC-Chol for the L_o phase with [Chol] = 40% at 48 °C.⁴ From the top to the bottom on the left side, they, respectively, represent the approximate absorption spectra as a normalized contour plot,⁵ as a stack plot, and the simulated absorption spectra using the best-fit parameters of the full S_{c-} results. The equivalent results are shown on the right side for the magnitude spectra. The simulation parameters [29] are: $R_{\perp} = 8.2 \times 10^8$ s⁻¹, $R_{\parallel} = 11.5 \times 10^9$ s⁻¹, $S_0 = 0.3$, $S_2 = -0.3$, $\Delta = 0.7$ G, $T_{2,edi} = 328$ ns.

The approximate pure absorption spectra as normalized contour plots⁵ (top left) and stack plots (middle left) were obtained directly from experiment using the results of the phase factors obtained in the full S_{c-} fitting. Their respective magnitude-mode representations of the experiments (top and middle right in Fig. 5), and the simulated pure absorption and magnitude spectra (bottom of Fig. 5) using the best-fit parameters in the full S_{c-} domain are also shown in Fig. 5 for comparison. It is clear that the spectral resolution is significantly increased in the absorption mode, as comparing the recovered absorption spectra to the magnitude-mode spectra. In the absorption mode, the line-shapes along the f_1 axis are in principle a sum of

Lorentzians with simple homogeneous linewidths (cf. Eq. (9) with Eq. (5)). The T_2^{-1} variation of the HB, which is obscured in the magnitude mode, becomes clear even by visual inspection of the absorption spectra displayed as normalized contour plots [12,13].

A comparison of the approximate absorption and magnitude spectra with their respective best fits, while good, does show some differences. We attribute them to (i) the approximate nature of the experimental absorption spectra and (ii) the use of a simple model for the molecular dynamics, (i.e. the MOMD model). Such differences are greater for the gel phase, which has always posed a greater challenge in analysis [6,9,10].

To demonstrate the benefits provided by the high-resolution absorption spectra for studying the coexistence of membrane phases, we show in Fig. 6 two simulated absorption (normalized) spectra, which represent the coexisting L_o and gel phases at 25 °C, as well as their respective dynamic parameters. Note that the best-fit dynamic

⁵ Normalized contours are obtained from the 2D-ELDOR spectra in the SECSY format by first dividing them by the $\omega_1 = 0$ slice. That is they are obtained from: $S_c^{\text{SECSY}}(\omega_1, T_m, \omega_2) / S_c^{\text{SECSY}}(\omega_1 = 0, T_m, \omega_2)$. This normalized format is useful for illustrating the homogeneous linewidths as a function of ω_2 [33].

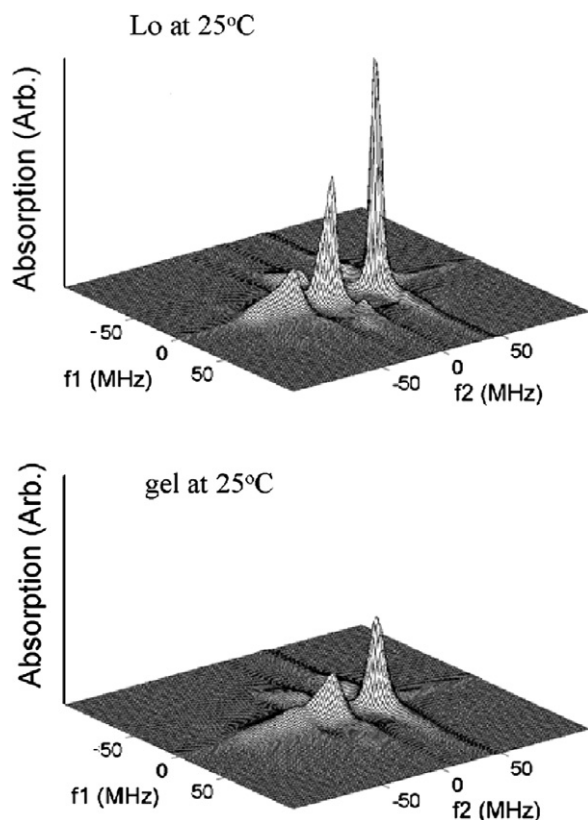


Fig. 6. The simulated absorption spectra ($T_m = 50$ ns, $t_{d1,2} = 0$ ns) for the two spectral components, corresponding to the L_o and the gel phases, which coexist for [Chol] \sim 20–30% in the DPPC–cholesterol binary system at 25 °C using 16PC. The best fit simulation parameters [29] for the L_o and the gel phases, respectively, are: $R_{\perp} = 3.1 \times 10^8$ s $^{-1}$, $R_{\parallel} = 7.4 \times 10^9$ s $^{-1}$, $S_0 = 0.3$, $S_2 = -0.2$, $\Delta = 0.45$ G, $T_{2,edi} = 336$ ns. and $R_{\perp} = 1.3 \times 10^8$ s $^{-1}$, $R_{\parallel} = 2.1 \times 10^9$ s $^{-1}$, $S_0 = 0.38$, $S_2 = -0.4$, $\Delta = 0.98$ G, $T_{2,edi} = 252$ ns.

parameters were obtained using full S_{c-} fitting. This enabled us to perform an accurate decomposition of the two component 2D-ELDOR spectra from the coexistence region, despite similarities in these two phases. The L_o spectral component displays a sharper lineshape than the gel spectral component (cf. Fig. 6). The spectra we obtained at 20% and 30% [Chol] consist of 15% and 90% of the L_o spectral component, respectively, with the remainder due to the gel component. Both spectral components are found to possess high ordering; but the L_o component is characteristic of faster molecular motion, while the gel component is characterized by slower molecular motion. This example illustrates how 2D-ELDOR, especially in the pure absorption representation, clearly distinguishes between the L_o and gel phases, which differ only subtly in their respective dynamic and structural properties.

3.2. Biomembrane study: PMV from RBL-2H3 mast cells

One of the first descriptions of the phase structure changes in biomembranes upon external stimulation has been achieved using 2D-ELDOR techniques by Freed and co-workers [13]. The physical characterization of bio-

membrane properties, e.g. phase molecular structures, phase coexistence, and microdomain sizes, is of great interest in biophysics and biochemistry. Several physical chemistry methods have been useful in investigating membrane phases, e.g. fluorescence spectroscopy [36], NMR [37,38], single particle tracking [39], and ESR. However, the local heterogeneity and complexity in the phase environment of biomembranes has posed a challenge to the existing physical methods. Among these techniques, ESR provides several unique features, such as the capability of providing both spectroscopic evidence and quantitative descriptions for the molecular dynamic structures, as we have recently demonstrated in the studies of model [10,12,14,16] and biological [13,14,18] membranes.

Using the full S_{c-} method, we have been able to investigate membrane phase structure changes with respect to temperature variations, as well as those caused by external stimulation to the cells (i.e. cross-linking of Immunoglobulin E (IgE) receptors on the surface of the membrane vesicles) [13]. Here, we emphasize how the great sensitivity of 2D-ELDOR and the full S_{c-} method lead to a powerful method for the study of complex biomembranes.

In the study of plasma membrane vesicles (PMV) isolated from the RBL-2H3 mast cells, we find that [13] (i) there are two major spectral components with spectral characteristics of L_o and L_d phases, which differ mainly in their ordering and coexist in the PMV both before and after stimulation; (ii) upon stimulation (i.e. crosslinking of the IgE receptors on the surface of PMV), the observed small but significant spectral changes are due to the remodeling of the membrane environment toward being more disordered. The unambiguous fits in both ELDOR and SECSY formats in the full S_{c-} domain enable the accurate characterization of the subtle spectral changes in these two-component spectra. (Attempts at using the magnitude spectra were not very successful at converging to these differences.)

We now illustrate the advantages of using 2D-ELDOR with the full S_{c-} method. Fig. 7 compares the (approximate) absorption spectra and the normalized spectra ($T_m = 50$ ns) in the SECSY format for the unstimulated and stimulated samples at 30 °C.⁴ These are presented as normalized contour plots⁵ (upper figures) and stack plots (middle figures). In addition they show (at the bottom) the simulated absorption spectra using the best-fit parameters obtained from the full S_{c-} fits. It is clear from the absorption spectra, which have a better resolution than the magnitude-mode spectra, that upon stimulation there are small but significant changes in the spectra. Such changes, analyzed by spectral simulations in the full S_{c-} domain, are found to be mainly due to the remodeling of the PMV by a decrease in the more ordered L_o component and an increase in the disordered L_d component, although the former is still the major component in the PMV, before and after stimulation. Although we only show the case of $T_m = 50$ ns in Fig. 7, it is worth mentioning that weak cross-peak development is observed (though negative; cf.

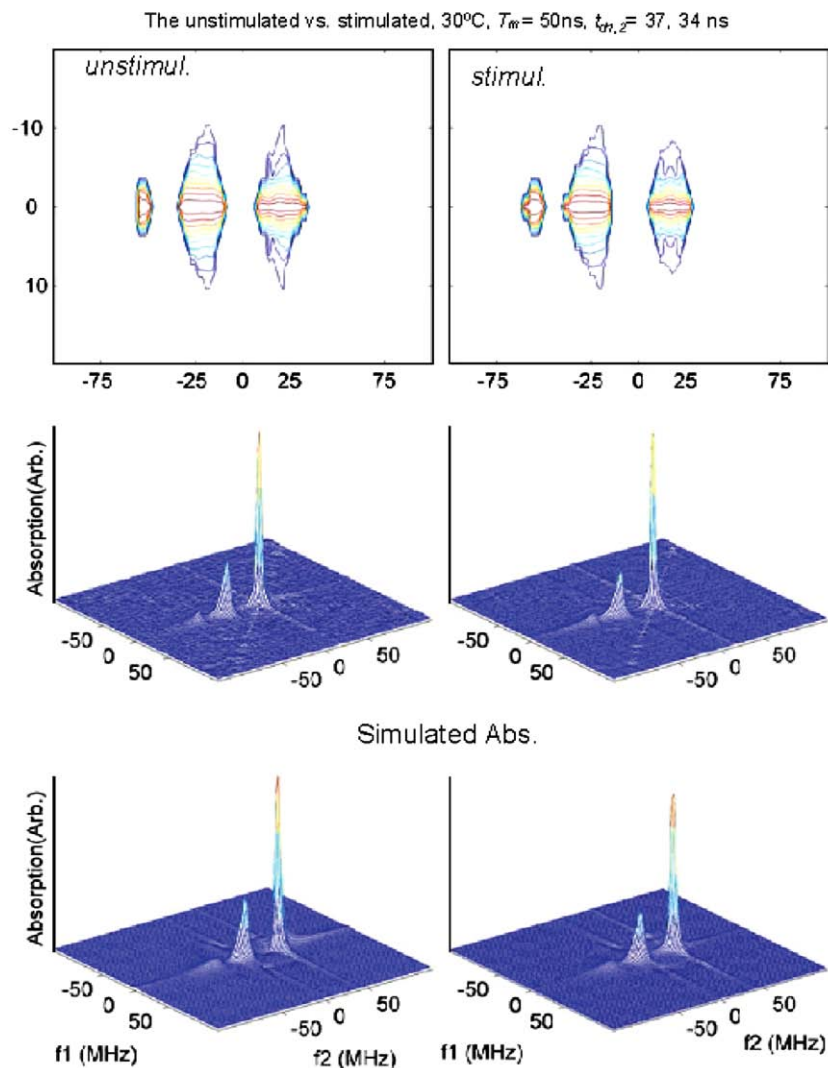


Fig. 7. The 2D-ELDOR spectra ($T_m = 50$ ns) in the SECSY format for 16PC in the unstimulated (left column) and the stimulated (right column) PMV's at 30 °C.⁴ From the top to the bottom in each column, they respectively represent the approximate absorption spectra as a normalized contour plot, as a stack plot, and the simulated absorption spectra using the best-fit parameters of the full S_{c-} results. The simulation parameters [29] for the L_d component (the L_o component) are: Unstimulated: $R_{\perp} = 4.4(4.6) \times 10^8 \text{ s}^{-1}$, $R_{\parallel} = 3.4(9.1) \times 10^9 \text{ s}^{-1}$, $S_0 = 0.10(0.25)$, $S_2 = -0.21(-0.27)$, $\Delta = 0.1(0.4)$ G, $T_{2,\text{edi}} = 622(302)$ ns. Stimulated: $R_{\perp} = 3.0(3.9) \times 10^8 \text{ s}^{-1}$, $R_{\parallel} = 2.3(7.9) \times 10^9 \text{ s}^{-1}$, $S_0 = 0.07(0.23)$, $S_2 = -0.33(-0.32)$, $\Delta = 0.05(0.40)$ G, $T_{2,\text{edi}} = 730(1, 352)$ ns.

Fig. 4d) in the recovered absorption spectra of the unstimulated and stimulated samples for the longest mixing times ($T_m \sim 400$ and 1200 ns). Such cross-peak development is not observed in the model studies for both the pure gel and L_o phases (e.g. $t_d > 28$ ns; cf. Fig. 6), as we have noted above. This cross-peak development, therefore, is considered to be evidence for the existence of a small amount of the L_d component in the PMV. Such evidence cannot be obtained if the spectra are displayed in the magnitude mode, and is only revealed in the absorption-mode spectra with long mixing time.

Fig. 8 shows the simulated pure absorption spectra, which are obtained using the best-fit parameters of the full S_{c-} fits, with $T_m = 50$ ns (and for zero dead-time) for the two coexisting spectral components, due to the L_o and the L_d membrane regions, at 30 °C. These two plots clearly

demonstrate that the L_d component is responsible for the cross-peaks development at $T_m = 50$ ns. As T_m increases, the cross-peaks of both components are found to grow significantly but with different developing rates. The cross-peak development vs. T_m for the L_d component is always found to be much greater than that of the L_o component. Such cross-peak development is consistent with the results obtained in the model membrane study.

4. Summary and conclusions

We have reported the improved capability and sensitivity of 2D-ELDOR techniques provided by the full S_{c-} method, in capturing the molecular dynamics in membrane systems. The new method doubles the fitting dimensions by extending the fitting domain from the magnitude mode to

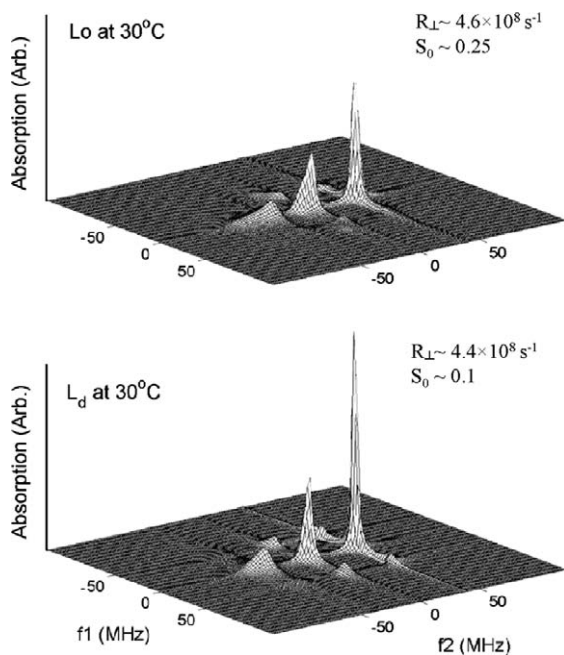


Fig. 8. The simulated absorption spectra ($T_m = 50$ ns, $t_{d1,2} = 0$ ns) for the two spectral components, L_o and L_d , coexisting in the unstimulated PMV samples of the RBL-2H3 mast cells at 30 °C. The best-fit simulation parameters are given in the caption to Fig. 7.

the full S_{c-} mode, i.e. simultaneously fitting the real and imaginary parts of the S_{c-} signal. Three phase correction factors are included into the analysis to approximate the effects of experimental artifacts, such as imperfect pulse shapes and imperfect bandwidth coverage. The phase factors as well as the dynamic parameters are accurately recovered. In addition, the phase correction factors may be used to recover an (approximate) 2D absorption spectrum from the experimental data, and it is characterized by high spectral resolution.

The new method has been tested in a study of DPPC–cholesterol binary mixtures to demonstrate its improved capability. The great sensitivity of 2D-ELDOR emphasizes the subtle differences of the gel, L_o and L_d phases. In a study of a biomembrane, the new method proved useful in discerning the small but significant spectral changes which are observed upon crosslinking of IgE receptors on the surface of the plasma membrane vesicles of RBL-2H3 cells. The fits in the full S_{c-} domain are unambiguous and are useful for characterizing the domain structures of PMV.

Acknowledgments

This project was supported by grant number P41RR16292 from the National Center for Research Resource (NCR), and grant number R01EB03150 from the National Institute of Biomedical Imaging and Bioengineering, components of the National Institute of Health (NIH), and its contents are solely the responsibility of the authors and do not necessarily represent the official view

of NCR or NIH. Computations were implemented at the Cornell Center for Materials Research Computing Facility. We wish to thank Barbara Baird and David Holowka for the plasma membrane vesicle samples.

References

- [1] J. Gorcoster, J.H. Freed, Two-dimensional Fourier-transform electron-spin-resonance correlation spectroscopy, *J. Chem. Phys.* 88 (1988) 4678–4693.
- [2] J. Gorcoster, J.H. Freed, Two-dimensional Fourier-transform electron-spin-resonance spectroscopy, *J. Chem. Phys.* 85 (1986) 5375–5377.
- [3] J. Gorcoster, S.B. Rananavare, J.H. Freed, Two-dimensional electron electron double-resonance and electron-spin echo study of solute dynamics in smectics, *J. Chem. Phys.* 90 (1989) 5764–5786.
- [4] S. Saxena, J.H. Freed, Two-dimensional electron spin resonance and slow motions, *J. Phys. Chem. A* 101 (1997) 7998–8008.
- [5] D.J. Xu, R.H. Crepeau, C.K. Ober, J.H. Freed, Molecular dynamics of a liquid crystalline polymer studied by two-dimensional Fourier transform and CW ESR, *J. Phys. Chem.* 100 (1996) 15873–15885.
- [6] S. Lee, B.R. Patyal, S. Saxena, R.H. Crepeau, J.H. Freed, Two-dimensional Fourier-transform electron spin resonance in complex fluids, *Chem. Phys. Lett.* 221 (1994) 397–406.
- [7] R.H. Crepeau, S. Saxena, S. Lee, B. Patyal, J.H. Freed, Studies on lipid-membranes by 2-dimensional fourier-transform ESR - enhancement of resolution to ordering and dynamics, *Biophys. J.* 66 (1994) 1489–1504.
- [8] S.Y. Lee, D.E. Budil, J.H. Freed, Theory of 2-dimensional Fourier-transform electron-spin-resonance for ordered and viscous fluids, *J. Chem. Phys.* 101 (1994) 5529–5558.
- [9] B.R. Patyal, R.H. Crepeau, J.H. Freed, Lipid-gramicidin interactions using two-dimensional Fourier-transform electron spin resonance, *Biophys. J.* 73 (1997) 2201–2220.
- [10] A.J. Costa-Filho, Y. Shimoyama, J.H. Freed, A 2D-ELDOR study of the liquid ordered phase in multilamellar vesicle membranes, *Biophys. J.* 84 (2003) 2619–2633.
- [11] A.J. Costa-Filho, R.H. Crepeau, P.P. Borbat, M. Ge, J.H. Freed, Lipid-gramicidin interactions: dynamic structure of the boundary lipid by 2D-ELDOR, *Biophys. J.* 84 (2003) 3364–3378.
- [12] Y.-W. Chiang, A.J. Costa-Filho, J.H. Freed, Molecular dynamic structure and phase diagram of DPPC–cholesterol binary mixtures: A 2D-ELDOR study, *J. Phys. Chem. B.* (2007), in press.
- [13] Y.-W. Chiang, A.J. Costa-Filho, D. Holowka, B. Baird, J.H. Freed, 2D-ELDOR for biomembranes: crosslinking IgE receptors causes phase structure changes in plasma membrane vesicles, in preparation.
- [14] M. Ge, A. Gidwani, H.A. Brown, D. Holowka, B. Baird, J.H. Freed, Ordered and disordered phases coexist in plasma membrane vesicles of RBL-2H3 mast cells. An ESR study, *Biophys. J.* 85 (2003) 1278–1288.
- [15] M.T. Ge, J.H. Freed, Hydration, structure, and molecular interactions in the headgroup region of dioleoylphosphatidylcholine bilayers: an electron spin resonance study, *Biophys. J.* 85 (2003) 4023–4040.
- [16] Y.-W. Chiang, Y. Shimoyama, G.W. Feigenson, J.H. Freed, Dynamic molecular structure of DPPC–DLPC–cholesterol ternary lipid system by spin-label electron spin resonance, *Biophys. J.* 87 (2004) 2483–2496.
- [17] B.G. Dzikovski, P.P. Borbat, J.H. Freed, Spin-labeled gramicidin A: channel formation and dissociation, *Biophys. J.* 87 (2004) 3504–3517.
- [18] M.J. Swamy, L. Ciani, M. Ge, A.K. Smith, D. Holowka, B. Baird, J.H. Freed, Coexisting domains in the plasma membranes of live cells characterized by spin-label ESR spectroscopy, *Biophys. J.* 90 (2006) 4452–4465.
- [19] S.Y. Kang, H.S. Gutowsky, J.C. Hsung, R. Jacobs, T.E. King, D. Rice, E. Oldfield, Nuclear magnetic-resonance investigation of the cytochrome oxidase-phospholipid interaction – new model for boundary lipid, *Biochemistry* 18 (1979) 3257–3267.

- [20] P.C. Jost, O.H. Griffith, R.A. Capaldi, G. Vanderko, Evidence for boundary lipid in membranes, *Proc. Natl. Acad. Sci. USA* 70 (1973) 480–484.
- [21] J.P. Hornak, J.H. Freed, Spectral rotation in pulsed electron-spin-resonance spectroscopy, *J. Mag. Res.* 67 (1986) 501–518.
- [22] J. Gorcester, G.L. Millhauser, J.H. Freed, Two-dimensional electron spin resonance, in: L. Kevan, M.K. Bowman (Eds.), *Modern Pulsed and Continuous Wave Electron Spin Resonance*, Wiley, New York, 1990, pp. 119–194, Ch. 3.
- [23] M.K. Bowman, Fourier transform electron spin resonance, in: L. Kevan, M.K. Bowman (Eds.), *Modern Pulsed and Continuous Wave Electron Spin Resonance*, Wiley, New York, 1990 (Chapter 1).
- [24] J.M. Fauth, S. Kababya, D. Goldfarb, Application of 2D FT-EPR spectroscopy to study slow intramolecular chemical exchange, *J. Mag. Res.* 92 (1991) 203–207.
- [25] M. Pluschau, K.P. Dinse, 2D EPR study of a photoinduced proton abstraction in the system anthraquinone and 4-methyl-2,6-di-tert-butylphenol in 2-propanol, *J. Mag. Res., Ser. A* 109 (1994) 181–191.
- [26] P.P. Borbat, R.H. Crepeau, J.H. Freed, Multifrequency two-dimensional Fourier transform ESR: an X/Ku-band spectrometer, *J. Magn. Reson.* 127 (1997) 155–167.
- [27] J.H. Freed, Theory of slow tumbling ESR spectra for nitroxides, in: L.J. Berliner (Ed.), *Spin Labeling: Theory and Applications*, Academic Press, New York, 1976, pp. 53–132.
- [28] D.J. Schneider, J.H. Freed, Calculating slow motional magnetic resonance spectra. A user's guide, in: L.J. Berliner, J. Reuben (Eds.), *Spin Labeling: Theory and Application*, Plenum, New York, 1989, pp. 1–76.
- [29] D.E. Budil, S. Lee, S. Saxena, J.H. Freed, Nonlinear-least-squares analysis of slow-motion EPR spectra in one and two dimensions using a modified Levenberg-Marquardt algorithm, *J. Mag. Res. Ser. A* 120 (1996) 155–189.
- [30] B.R. Patyal, R.H. Crepeau, D. Gamliel, J.H. Freed, 2-Dimensional Fourier-transform ESR in the slow-motional and rigid limits- 2D-ELDOR, *Chem. Phys. Lett.* 175 (1990) 453–460.
- [31] D. Gamliel, J.H. Freed, Theory of 2-dimensional ESR with nuclear modulation, *J. Magn. Reson.* 89 (1990) 60–93.
- [32] J. Gorcester, J.H. Freed, Linear prediction and projection of pure absorption lineshapes in two-dimensional Ftesr correlation spectroscopy, *J. Mag. Res.* 78 (1988) 292–301.
- [33] S. Saxena, J.H. Freed, Absorption lineshapes in two-dimensional electron spin resonance and the effects of slow motions in complex fluids, *J. Magn. Reson.* 124 (1997) 439–454.
- [34] V.S.S. Sastry, A. Polimeno, R.H. Crepeau, J.H. Freed, Studies of spin relaxation and molecular dynamics in liquid crystals by two-dimensional Fourier transform electron spin resonance. 1. Cholestane in butoxy benzylidene-octylaniline and dynamic cage effects, *J. Chem. Phys.* 105 (1996) 5753–5772.
- [35] A. Polimeno, J.H. Freed, Slow motional ESR in complex fluids – the slowly relaxing local-structure model of solvent cage effects, *J. Phys. Chem.* 99 (1995) 10995–11006.
- [36] A.T. Hammond, F.A. Heberle, T. Baumgart, D. Holowka, B. Baird, G.W. Feigenson, Crosslinking a lipid raft component triggers liquid ordered-liquid disordered phase separation in model plasma membranes, *Proc. Natl. Acad. Sci. USA* 102 (2005) 6320–6325.
- [37] S.R. Shaikh, A.C. Dumaul, A. Castillo, D. LoCascio, R.A. Siddiqui, W. Stillwell, S.R. Wassall, Oleic and docosahexaenoic acid differentially phase separate from lipid raft molecules: A comparative NMR, DSC, AFM, and detergent extraction study, *Biophys. J.* 87 (2004) 1752–1766.
- [38] G. Oradd, P.W. Westerman, G. Lindblom, Lateral diffusion coefficients of separate lipid species in a ternary raft-forming bilayer: A Pfg-NMR multinuclear study, *Biophys. J.* 89 (2005) 315–320.
- [39] A. Kusumi, C. Nakada, K. Ritchie, K. Murase, K. Suzuki, H. Murakoshi, R.S. Kasai, J. Kondo, T. Fujiwara, Paradigm shift of the plasma membrane concept from the two-dimensional continuum fluid to the partitioned fluid: High-speed single-molecule tracking of membrane molecules, *Ann. Rev. Biophys. Biomol. Struct.* 34 (2005) 351–354.